International Journal of Control

ISSN: (Print) (Online) Journal homepage: https://www.tandfonline.com/loi/tcon20

Discrete-time data-driven control with Hölder-continuous real-time learning

A. K. Sanyal

To cite this article: A. K. Sanyal (2021): Discrete-time data-driven control with Hölder-continuous real-time learning, International Journal of Control, DOI: 10.1080/00207179.2021.1901993

To link to this article: https://doi.org/10.1080/00207179.2021.1901993

Published online: 19 Mar 2021.

INTERNATIONAL JOURNAL OF CONTROL
https://doi.org/10.1080/00207179.2021.1901993

Taylor & Francis
Taylor & Francis Group

Discrete-time data-driven control with Hölder-continuous real-time learning

A. K. Sanyal

Mechanical and Aerospace Engineering, Syracuse University, Syracuse, NY, USA

ABSTRACT

This work provides a framework for data-driven control of discrete-time systems with unknown dynamics and outputs controllable by the inputs. This framework leads to stable and robust real-time control such that a feasible output trajectory can be tracked. This is made possible by Hölder-continuous real-time stable learning schemes that act as discrete-time stable uncertainty observers. These observers learn from prior input-output history and ensure finite-time stable convergence of estimation errors to a bounded neighborhood of the zero vector if the system is Lipschitz-continuous with respect to time, outputs, inputs, internal parameters and states. In combination with nonlinearly stable controllers, this makes the proposed framework nonlinearly stable and robust to disturbances, model uncertainties, and unknown measurement noise. Nonlinear stability and robustness analyses of the observer and controller designs are carried out using discrete Lyapunov analysis. A numerical experiment on a second-order system demonstrates the performance of this nonlinear model-free control framework.

ARTICLE HISTORY
Received 10 June 2020
Accepted 7 March 2021

KEYWORDS
Data-driven control; finite-time stabilisation; Hölder-continuous feedback; uncertainty observer

1. Introduction

Data-driven control approaches are used for feedback control of systems with uncertain or unknown input–output behaviour. When only input–output behaviour of the system is observable, then output regulation to a desired set point or output trajectory tracking has to be based on data-driven (model-free) controller and observer designs. This work provides a nonlinear data-driven control framework for output tracking of systems for which the measured output variables can be controlled by the applied inputs, but the model describing the input–output relation is unknown or uncertain. The main contribution of this work is that it provides definite (quantifiable) guarantees on nonlinear stability and robustness in real-time learning of the unknown input–output dynamics and controlling the output along feasible prescribed trajectories.

A majority of linear and nonlinear control approaches are model-based for which a model of the dynamics of the system being controlled is necessary. However, as the number and variety of systems to which control theory is applied increases, uncertainties and difficulties in modelling need to be overcome. Of particular interest to this work is the large class of (nonlinear) systems with uncertain or unmodelled dynamics that have to be controlled in real-time. This class of systems includes, for example, autonomous vehicles, walking robots, and electronic medical implants. For such systems, data-driven (i.e. model-free) control techniques may be used for feedback control in real-time. The term 'model-free control' for uncertain systems has been used in different senses and settings in the published literature. These settings are quite varied, and range from 'classic' PIDs to feedback control using techniques from neural nets, fuzzy logic, and soft computing to learn the uncertainties in the dynamics, e.g. in Keel and Bhattacharya (2017), Killingsworth and Krstic (2006), dos Santos Coelho et al. (2010), Syafiie et al. (2011), Ren and Bigras (2017). A model-free control framework based on classical control, termed the 'intelligent PID' (or 'iPID') scheme, was proposed in Fliess et al. (2008) and Fliess and Join (2013). The iPID framework uses an *ultra-local model* to describe the unknown input–output dynamics, and estimates and uses this model for feedback control. In addition, if the system is known to be differentially flat for the selected outputs (Fliess et al., 1995), then a state trajectory can also be tracked and uncertainties in the input-state dynamics can also be estimated over time from the measured outputs using model-free filtering techniques (Fliess et al., 2008; Trapero et al., 2007). However, in the iPID framework, the ultra-local model is estimated by a linear filtering scheme assuming measurements at a sufficiently high sampling frequency (Mboup et al., 2009; Tabuada et al., 2017). Some applications where similar model-free control techniques have been considered are given in, e.g. Roman et al. (2017), Younes et al. (2016), Villagra and Balaguer (2011) and Y. Chang et al. (2011). More recently, a data-enabled predictive control ('DeePC') method was formulated for data-driven control of unmodelled/uncertain systems that is analogous to the classical model-predictive control (MPC) technique for model-based control of linear systems in Coulson et al. (2019). Data-driven control algorithms that use disturbance or uncertainty observers and maintain input constraints have also been treated, e.g. in Polóni et al. (2014) and Polóni

CONTACT A. K. Sanyal aksanyal@syr.edu Mechanical and Aerospace Engineering, Syracuse University, Syracuse, NY 13244, USA

et al. (2017). Other recent data-driven control schemes based on linear systems theory include (Novara & Formentin, 2018; Tabuada & Fraile, 2019). *However, none of these data-driven control techniques guarantee nonlinear stability and robustness in discrete-time.* Guaranteed robustness and nonlinear stability in the sense of Lyapunov (1992) is required for wider applicability and reliability of data-driven control approaches for systems with modelling uncertainties and unknowns.

While most prior work has used continuous-time feedback for data-driven control, the framework developed here uses discrete-time Hölder-continuous nonlinear model-free estimation and control for tracking desired output trajectories. The main reason for the development of this framework here in discrete time is because that makes it easier to implement numerically and experimentally. This discrete-time framework is implementable on embedded processors for real-time applications like autonomous vehicles and robotics. In addition, the discrete-time representation of an unknown system with known relative degree between inputs and outputs 'naturally' accounts for time the delay in the input–output system. This is because the (unknown) discrete-time input–output system representation considers the output as dependent on inputs and outputs from previous sampling instants. This framework lays the foundation for nonlinearly stable and robust data-driven control in discrete time, using novel methods to estimate the local input–output model and for tracking control. Our past research using Hölder-continuous finite-time stable control and estimation schemes in continuous time have appeared in, e.g. Bohn and Sanyal (2015), Viswanathan et al. (2017), Sanyal, Warier, and Hamrah (2019) and Sanyal, Warier, and Viswanathan (2019). The finite-time stable uncertainty and output observers can be designed to converge in a finite time period that is smaller than the settling time of the controller. For tracking the desired output or state trajectory, a Hölder-continuous nonlinear finite-time stable (FTS) tracking control scheme was used in Bohn and Sanyal (2015) and Viswanathan et al. (2017). These FTS schemes are based on the Lyapunov analysis in Bhat and Bernstein (2000), using Hölder-continuous Lyapunov functions. More recently, we developed a discrete-time version of these FTS schemes and used it for tracking control (Hamrah et al., 2019). Here, we extend this basic discrete-time analysis to provide finite-time stable learning of unknown dynamics in real-time. *The resulting framework for data-driven control provides guaranteed nonlinear stability of the overall feedback system without requiring high frequencies for measurement or control.* The overall emphasis in our approach is towards *guaranteeing nonlinear stability and robustness of the feedback system* using FTS learning of unknown dynamics. This follows up on our recent preliminary work (C. Chang et al., 2020), which developed a continuous-time version of this work and applied it to functional electrical stimulation of muscles. Unlike this preliminary work which considered only relative degree one (first-order) input–output dynamics and had an asymptotically stable tracking controller, here we develop a general framework in discrete time, that applies to any relative degree between inputs and outputs and provides finite-time stability of the feedback system with respect to uncertainty estimation errors and tracking errors.

In the first part of our nonlinear model-free control framework, basic theoretical results on nonlinear Hölder-continuous finite-time stabilisation in discrete time are developed. The second part of our framework uses these results to design two nonlinearly stable and robust observers that predict the unknown model describing the input–output dynamics locally in state-space and time, based on prior observed input–output behaviour. This is a critical component of our framework, as these observers work as uncertainty observers that are used to compensate for the unknown dynamics and ensure nonlinear stability of the overall feedback loop. In the third part of this framework, we design a nonlinearly stable, trajectory tracking control scheme to track the desired output trajectory. This nonlinearly stable control scheme ensures convergence of the output tracking error to zero in finite time if the uncertainty estimates are perfect. It is shown to be nonlinearly stable and robust to bounded errors in the uncertainty estimates. Further, if these estimates are obtained from the uncertainty observers designed in the second part of our framework, we show that the tracking errors are guaranteed to converge to a neighbourhood of zero.

The remainder of this paper is organised as follows. The mathematical formulation and assumptions on discrete-time nonlinear systems along with the theory of Hölder-continuous finite-time stability in discrete time, are developed in Section 2. The basic result stated in Lemma 2.1 first appeared in Hamrah and Sanyal (2020). The remaining analytical results in this paper, including Theorem 2.1 in Section 2, have not appeared before. In Section 3, two finite-time stable uncertainty observers are designed to estimate the unknown local model relating the inputs and outputs of the nonlinear system. This model relates the observed outputs of the system to the given inputs, and accounts for the combined effects of unknown internal states and unknown external inputs (uncertainties). This is another novel contribution of this paper. Two novel model-free control laws for output tracking are given in Section 4. These discrete time control laws make the feedback system converge to the desired output trajectory in a finite-time stable manner if the estimated model converges exactly to the true input–output dynamics. Section 5 provides numerical simulation results of applying this nonlinear model-free control framework to output trajectory tracking of a two-degree of freedom mechanical system. The model of the system is assumed to be unknown for purposes of control design, and it includes nonlinear friction terms affecting the dynamics of both degrees of freedom. The results of this numerical simulation agree with the analytical stability and robustness properties of this control framework. Finally, Section 6 provides a summary of the main results and ends with planned future work.

2. Nonlinear system assumptions and finite-time stability in discrete time

In the first part of this section, we lay out the assumptions on discrete nonlinear systems for which the proposed framework of data-driven control are applicable. In the second part of this section, we give a result on the finite-time stability of such discrete nonlinear systems.

2.1 Assumptions on discrete nonlinear system for our framework of data-driven control

Consider a discrete nonlinear system with m inputs, n outputs, and l unknown internal parameters or states. We denote by $\mathbb{R}$ the set of all real numbers, $\mathbb{R}^+$ the set of all positive numbers, and $\mathbb{R}_0^+$ the set of all non-negative numbers. The notation $(\cdot)_k = (\cdot)(t_k)$ denotes the value of a time-varying quantity at sampling instant $t_k \in \mathbb{R}_0^+$, with $u_k \in \mathbb{R}^m$ as the input vector comprising control inputs, $y_k \in \mathbb{R}^n$ is the output vector consisting of measured output variables, and $z_k \in \mathbb{R}^l$ is the vector of unknown (unobservable) internal parameters and states. Here, $k \in \mathbb{W} = \{0, 1, 2, \ldots\}$ and $\mathbb{W}$ is the index set of whole numbers including 0.

We use the superscript (μ) to denote the μth order finite difference of a quantity in discrete time. The forward difference defined by

$$y_k^{(\mu)} := y_{k+1}^{(\mu-1)} - y_k^{(\mu-1)} \quad \text{with } y_k^{(0)} = y_k \tag{1}$$

is used here, because of its simplicity and applicability. Let ν be the relative degree of the input–output system. The unknown discrete system can be expressed as

$$y_k^{(\nu)} = \varpi(y_k, y_k^{(1)}, \ldots, y_k^{(\nu-1)}, z_k, u_k, t_k), \tag{2}$$

where ϖ is unknown, and $y_k^{(\mu)}$ is the μth order finite difference defined by Equation (1). Using Equation (1), we can alternately represent the system (2) as

$$y_{k+\nu} = \varphi(y_k, y_{k+1}, \ldots, y_{k+\nu-1}, z_k, u_k, t_k). \tag{3}$$

Note that $\varpi, \varphi : (\mathbb{R}^n)^\nu \times \mathbb{R}^l \times \mathbb{R}^m \times \mathbb{R}_0^+ \to \mathbb{R}^n$ are possibly time-varying but unknown or imperfectly known. The control inputs u_k are then designed so as to track a desired output trajectory $y_k^d = y^d(t_k)$. The following basic assumptions are made in order to have a tractable discrete-time output tracking control problem.

Assumption 2.1: *The discrete-time nonlinear system given by* (2) (*alternately* (3)) *has input–output dynamics* $\varpi(\cdots)$ (*alternately* $\varphi(\cdots)$) *that is unknown but Lipschitz continuous in all arguments.*

Assumption 2.2: *The matrix* $\mathsf{G}_k \in \mathbb{R}^{n\times m}$ *is always full ranked with* $m \geq n$*, so that the outputs can be controlled by the inputs. Further, inputs are applied simultaneously with output measurements at time instants* t_k.

Assumption 2.3: *The desired output trajectory* $y_k^d := y^d(t_k)$ *to be tracked by the discrete system* (2) (*alternately* (3)), *is obtained by sampling a continuous and* ν *times differentiable trajectory in time,* $y^d(t)$, *with bounded time derivatives up to order* ν.

Let $\chi_k = (y_k, y_{k+1}, \ldots, y_{k+\nu-1}, z_k, u_k, t_k)$ denote the vector of variables on which the system (3) depends. Then Assumption 2.1 implies that

$$\|y_{k+\nu+1} - y_{k+\nu}\| = L\|\chi_{k+1} - \chi_k\|, \tag{4}$$

where L is the Lipschitz constant. Further, $\varphi(\cdots)$ can be represented as

$$\varphi(\chi_k) = \mathsf{F}_k + \mathsf{G}_k u_k, \text{ where } \mathsf{F}_k = \mathsf{F}(\chi_k) \text{ and } \mathsf{G}_k = \mathsf{G}(\chi_k), \tag{5}$$

where $\mathsf{F} : \mathbb{R}^{n\nu} \times \mathbb{R}^l \times \mathbb{R}^m \times \mathbb{R}_0^+ \to \mathbb{R}^n$ and $\mathsf{G} : \mathbb{R}^{n\nu} \times \mathbb{R}^l \times \mathbb{R}^m \times \mathbb{R}_0^+ \to \mathbb{R}^{n\times m}$ are Lipschitz continuous in their arguments. Note that the unknown F and G may not be unique for a $\varphi(\cdots)$. When the relative degree ν is unknown, ν can be identified using known techniques (e.g. He & Asada, 1993; Rhodes & Morari, 1998), or a sufficiently high value that is larger than the unknown relative degree may be assumed for model-free control.

In practice, outputs are measured by sensors that usually introduce noise, modelled by

$$y^m(t_k) = y_k^m = y_k + \eta_k, \tag{6}$$

where $\eta_k \in \mathbb{R}^l$ is a vector of additive noise. A nonlinearly stable filtering scheme can be used to filter out this measurement noise. In particular, nonlinear finite-time stable observers can filter out noise and provide rapid convergence, as shown recently in Sanyal, Warier, and Hamrah (2019), Sanyal, Warier, and Viswanathan (2019) and Wang et al. (2019).

2.2 Finite-time stabilisation in discrete time using Hölder continuous feedback

This section gives a basic result on finite-time stability for discrete time systems that lead to an Hölder-continuous system. This result has the following benefits in our framework for model-free control: (1) the added robustness of finite-time stability compared to asymptotic stability for nonlinear systems when faced with the same intermittent or persistent disturbances (Bhat & Bernstein, 2000; Bohn & Sanyal, 2015); and (2) convergence to zero errors in finite time makes it easier to analyse stability and robustness of the feedback system after separate observer and controller designs. This basic result has recently appeared in Wang et al. (2019) and Hamrah et al. (2019). Here, we give the same result with a simpler mathematical proof, followed by a new result showing Hölder continuity of the system.

Lemma 2.1: *Consider a discrete-time system with outputs* $s_k \in \mathbb{R}^p$. *Let* $V : \mathbb{R}^p \to \mathbb{R}$ *be a positive definite, decrescent and radially unbounded (Lyapunov) function (Vidyasagar, 2002) of the outputs, and denote* $V_k := V(s_k)$. *Let* α *be a constant in the open interval* $]0, 1[$. *Denote* $\gamma_k := \gamma(V_k)$ *where* $\gamma : \mathbb{R}_0^+ \to \mathbb{R}_0^+$ *is a positive definite function of* V_k *that satisfies the condition that there exists* $\varepsilon \in \mathbb{R}^+$ *such that*

$$\gamma_k = \gamma(V_k) \geq \eta := \varepsilon^{1-\alpha} \quad \text{for all } V_k \geq \varepsilon. \tag{7}$$

Then, if V_k *satisfies the relation*

$$V_{k+1} - V_k \leq -\gamma_k V_k^\alpha, \tag{8}$$

the discrete system is stable at $s = 0$ *and* s_k *converges to* $s = 0$ *for* $k > N$, *where* $N \in \mathbb{W}$ *is finite.*

Proof: Clearly, inequality (8) is a sufficient condition for asymptotic stability of the zero output $s = 0$, as it ensures that the difference $V_{k+1} - V_k$ along output trajectories of the discrete-time system is negative definite. The right-hand side of the inequality (8) is zero if and only if $V_k = 0$, as $\gamma(\cdot)$ is a positive definite function of V_k. Therefore, the sequence $\{V_k\}$ is a monotonically decreasing sequence in $\mathbb{R}_0^+$. Combining condition (7) with inequality (8), we obtain

$$V_{k+1} \le V_k - \gamma_k V_k^\alpha \le V_k - \eta V_k^\alpha. \tag{9}$$

The rest of the proof uses contradiction to arrive at the given result. Note that V_k decreases at least as fast as the far right-hand side of the inequality (9). Now define

$$c_k := V_k/\varepsilon, \tag{10}$$

where $V_k = V(s_k)$ is the value of the Lyapunov function at time t_k. Substituting this expression for V_k in inequality (8), we obtain

$$\begin{aligned} V_{k+1} - c_k \eta^{\frac{1}{1-\alpha}} &\le -\eta c_k^\alpha (\eta)^{\frac{\alpha}{1-\alpha}} = -c_k^\alpha \eta^{\frac{1}{1-\alpha}} \\ \Rightarrow V_{k+1} &\le (c_k - c_k^\alpha)\eta^{\frac{1}{1-\alpha}} = (c_k - c_k^\alpha)\varepsilon. \end{aligned} \tag{11}$$

From Equation (10) $c_{k+1} := V_{k+1}/\varepsilon$, and from inequality (11):

$$c_{k+1} \le a_k \quad \text{where } a_k := c_k - c_k^\alpha. \tag{12}$$

Next, we consider two cases: (1) $c_k \le 1$; and (2) $c_k > 1$. In the first case, $c_{k+1} \le a_k \le 0$ from expression (12), as $\alpha \in]0, 1[$. Therefore, from (11) we get $V_{k+1} \le 0$. This leads to a contradiction because $V_{k+1} = V(s_{k+1})$ is a positive definite function of s_{k+1}. Therefore, $V_{k+1} = 0$ and as a result $s_{k+1} = 0$, which leads to convergence of the output s_j to the zero vector for all $j > N = k$.

In the second case, when $c_k > 1$, we see from Equation (12) that $c_{k+1} \le a_k$ and $a_k > 0$. Now, we repeat the previous few steps defined by expressions (10)–(12) by replacing $k \leftarrow k + 1$. As long as $c_j > 1 \Leftrightarrow a_j > 0$, this process can be continued to obtain monotonically decreasing sequences of positive real numbers $\{V_j\}$ and $\{c_j\}$ as follows:

$$V_{j+1} = c_{j+1}\varepsilon \quad \text{where } c_{j+1} \le a_j := c_j - c_j^\alpha,\ j \in \mathbb{W}. \tag{13}$$

Clearly, because $\alpha \in]0, 1[$, the sequence $\{c_j\}$ defined by Equation (13) is monotonically decreasing and $c_j \in \mathbb{R}^+$ for $c_j \ge 1$. Let $N \in \mathbb{W}$ $(N > k)$ be the smallest finite whole number such that $c_N \le 1$ (and correspondingly $a_N \le 0$) in this sequence. Therefore, $V_N = c_N\varepsilon \le \varepsilon = \eta^{\frac{1}{1-\alpha}}$ and $a_N = c_N - c_N^\alpha \le 0$. Then, from Equation (13), we have

$$V_{N+1} = c_{N+1}\varepsilon \le a_N\varepsilon \le 0.$$

As before, this leads to a contradiction as $V_{N+1} = V(s_{N+1})$ cannot be negative by definition; it has to be zero. Consequently, from the inequality (8), we see that $V_j = 0$ for $j \ge N + 1$. As a result, s_j converges to $s = 0$ for $j > N$. ■

Remark 2.1: Note that $\varepsilon \in \mathbb{R}^+$ is not given by this result; the result merely states that if such a positive ε exists that satisfies condition (7), then finite-time stability of $s = 0$ in discrete time is guaranteed. In fact, inequality (7) is easy to satisfy and holds true for all positive definite class-$\mathcal{K}$ functions $\gamma_k = \gamma(V_k)$. In particular, positive definite sigmoid functions are a good choice for $\gamma(V_k)$.

The result below shows the Hölder continuity of a Lyapunov function that satisfies condition (8) of Lemma 2.1.

Theorem 2.1: *A discrete-time Lyapunov function that satisfies inequality* (8) *is Hölder continuous in discrete time with exponent* $\frac{1}{1-\alpha}$.

Proof: From Lemma 2.1 and its proof, it is clear that $V_j > 0$ as long as $V_j > \varepsilon$. Further, it is also clear that $V_j = 0$ if $V_k \le \varepsilon$ for any $k < j$. Now consider indices $i, j \in \mathbb{W}$ such that $V_i, V_j > \varepsilon$ (i.e. $i, j < N$, where N is as defined in the proof of Lemma 2.1). Therefore, we have

$$\begin{aligned} V_{i+1} - V_0 &= V_{i+1} - V_i + V_i - V_{i-1} + \cdots + V_1 - V_0 \\ &\le -\eta(V_i^\alpha + \cdots + V_0^\alpha) < -(i+1)\eta V_{i+1}^\alpha \\ &\Rightarrow V_{i+1}^{1-\alpha} - \frac{V_0}{V_{i+1}^\alpha} < -(i+1)\eta, \end{aligned} \tag{14}$$

where we used the fact that $V_{i+1} < V_k$ for $k < i+1$. Rearranging inequality (14) and using $V_{i+1} > \varepsilon$, we have

$$\begin{aligned} V_{i+1} &< \left(\frac{V_0}{V_{i+1}^\alpha} - (i+1)\eta\right)^{\frac{1}{1-\alpha}} \\ &< (\upsilon - (i+1)\eta)^{\frac{1}{1-\alpha}}, \quad \text{where } \upsilon = \frac{V_0}{\varepsilon^\alpha}. \end{aligned} \tag{15}$$

A similar inequality holds if i is replaced by j in the expression above. Therefore, we conclude that

$$\frac{|V_{i+1} - V_{j+1}|}{|i-j|^{\frac{1}{1-\alpha}}} < \varepsilon + o(2) \tag{16}$$

using the fact that $\varepsilon = \eta^{\frac{1}{1-\alpha}}$, where $o(2)$ denotes second and higher order terms in $|i - j|$. Clearly, the above Hölder inequality holds trivially if either V_{i+1} or V_{j+1} or both are zero (i.e. $i \ge N$ and/or $j \ge N$). Therefore, the sequence $\{V_k\} \subset \mathbb{R}_0^+$ is Hölder-continuous in discrete time as given in the statement. ■

Remark 2.2: The statement of Theorem 2.1 for the Lyapunov function holds if the discrete-time system is replaced by a continuous-time system satisfying

$$\dot{V} \le -\eta V^\alpha,$$

for constant η as was shown in Theorem 4.3 of Bhat and Bernstein (2000). However, this Hölder continuity result for discrete-time systems has not appeared in prior publications, although it was presumed to be true in our earlier work (Hamrah & Sanyal, 2020; Wang et al., 2019).

The condition given in Lemma 2.1 can be satisfied easily for quadratic Lyapunov functions, as shown in the main result of the following section, which is in the form of a finite-time stable uncertainty observer in discrete time.

3. The ultra-local model and its estimation

In this section, we construct a control affine ultra-local model (ULM) in discrete time that models the unknown dynamics as an uncertain input to a control-affine system, and then estimates this uncertainty from past input–output data. We design first and second-order discrete-time nonlinear observers that estimate this uncertain input. Convergence to this uncertain input is achieved in finite time if this input is a constant vector; otherwise, these observers are shown to be robust to bounded rates of change of this uncertain input. This control-affine ULM along with the uncertainty observer is used in Section 4 to construct an output feedback control scheme to track the desired output trajectory.

3.1 Ultra-Local model for unknown system

The idea of an ultra-local model that is local in output (or state) space and in time, was proposed in the model-free control approach for SISO systems in Fliess and Join (2013). In this work, we generalise this concept to a discrete time nonlinear system with unknown dynamics of the form given by Equation (3), as follows:

$$y_{k+\nu} = \mathcal{F}_k + \mathcal{G}_k u_k, \quad \text{where } \mathcal{F}_k \in \mathbb{R}^n, \ u_k \in \mathbb{R}^m, \tag{17}$$

and $\mathcal{G}_k \in \mathbb{R}^{n\times m}$ is a full rank matrix that is designed or selected appropriately, as part of the controller design. Note that the $\mathcal{F}_k$ and $\mathcal{G}_k$ so obtained may not be unique and in particular, may not be equal to the F_k and G_k, respectively, in Equation (5), which is part of the Assumption 2.1 for the system (3). However, without any loss of generality, they can always be represented such that

$$\begin{aligned} \mathcal{F}_k &= \mathcal{F}(y_k, y_{k+1}, \dots, y_{k+\nu-1}, z_k, u_k, t_k), \\ \text{and} \quad \mathcal{G}_k &= \mathcal{G}(y_k, y_{k+1}, \dots, y_{k+\nu-1}, z_k, u_k, t_k). \end{aligned} \tag{18}$$

Further, based on Assumption 2.1, we can assume that

$$\begin{aligned} \|\mathcal{F}_{k+1} - \mathcal{F}_k\| &\le L_F \|\chi_{k+1} - \chi_k\|, \\ \|\mathcal{G}_{k+1} - \mathcal{G}_k\| &\le L_G \|\chi_{k+1} - \chi_k\|, \end{aligned} \tag{19}$$

where L_F and L_G are Lipschitz constants and χ_k is as defined before Equation (4).

The approach given here is centred around provable guarantees on nonlinear stability and robustness to the unknown dynamics. To do this in an effective manner, the unknown input–output dynamics, captured by $\mathcal{F}_k \in \mathbb{R}^n$ in Equation (17), should be estimated in a stable and robust manner. We, therefore, consider the following problem.

Problem 3.1: Consider the unknown nonlinear system (3) satisfying Assumptions 2.1, 2.2 and 2.3, with discrete control inputs $u_k := u(t_k) \in \mathbb{R}^m$ provided at sampling times t_k. Given the discrete time ultra-local model (17) of the input–output dynamics with unknown $\mathcal{F}_k$, estimate $\mathcal{F}_k$ from past input–output history and design a feedback control scheme to track the desired output trajectory $y_k^d := y^d(t_k)$ in a nonlinearly stable manner.

Note that as per Assumption 2.2, the system is input–output controllable. In the following subsections of this section, we design two nonlinear observers to estimate $\mathcal{F}_k$ for later use output feedback tracking control. These schemes (in isolation) can also be used to identify these unknown dynamics using known (feedforward) control inputs u_k and influence matrix $\mathcal{G}_k$. Note that this influence matrix $\mathcal{G}_k$ can also be designed to satisfy known control bounds, although we do not do that here.

3.2 Estimation of unknown input–output dynamics using a first order Observer

Note that the model given by (17) is a generalisation of the ultra-local model of Fliess and Join (2013), where $\mathcal{G}_k$ was a constant scalar and only single-input single-output (SISO) systems were considered. Here, we provide a first-order observer for this unknown dynamics, i.e. $\mathcal{F}_k$ in Equation (17). The idea here is to use the finite-time stable output observer design outlined in the previous section in conjunction with a first-order hold to estimate the unknown dynamics expressed by $\mathcal{F}_k$ in Equation (17) based on past input–output history. Note that the control law for u_k cannot use feedback of $\mathcal{F}_k$ which is unknown due to causality; but it can use an estimate of $\mathcal{F}_k$, denoted $\hat{\mathcal{F}}_k$ here, based on past information on $\mathcal{F}_j$ for $j \in \{0, \dots, k-1\}$. This approach is very different from the approach used in the iPID framework for continuous-time model-free control, which is based on numerical differentiation and estimation of derivatives from noisy signals in the Laplace domain (see Mboup et al., 2009).

Define the error in estimating $\mathcal{F}_k$ as follows:

$$e_k^{\mathcal{F}} := \hat{\mathcal{F}}_k - \mathcal{F}_k. \tag{20}$$

The following result gives a first order nonlinearly stable observer for the unknown dynamics $\mathcal{F}_k$.

Theorem 3.1: *Let $e_k^{\mathcal{F}}$ be as defined by Equation (20), and let $r \in \,]1,2[$ and $\lambda > 0$ be constants. Let the first order finite difference of the unknown dynamics $\mathcal{F}_k$, given by*

$$\Delta\mathcal{F}_k := \mathcal{F}_k^{(1)} = \mathcal{F}_{k+1} - \mathcal{F}_k \tag{21}$$

be bounded as in the first of Equations (19). Let the control influence matrix $\mathcal{G}_k$ be designed such that its first order finite difference is bounded as in the second of Equations (19). Consider the nonlinear observer for $\mathcal{F}_k$ given by

$$\begin{aligned} \hat{\mathcal{F}}_{k+1} &= \mathcal{D}(e_k^{\mathcal{F}})e_k^{\mathcal{F}} + \mathcal{F}_k \text{ given } \hat{\mathcal{F}}_0, \\ \text{where } \mathcal{D}(e_k^{\mathcal{F}}) &= \frac{((e_k^{\mathcal{F}})^{\mathrm{T}} e_k^{\mathcal{F}})^{1-1/r} - \lambda}{((e_k^{\mathcal{F}})^{\mathrm{T}} e_k^{\mathcal{F}})^{1-1/r} + \lambda}, \end{aligned} \tag{22}$$

and $\mathcal{F}_k = y_{k+\nu} - \mathcal{G}_k u_k$ according to the ultra-local model (17). This observer leads to finite time stable convergence of the estimation error vector $e_k^{\mathcal{F}} \in \mathbb{R}^l$ to a bounded neighbourhood of $0 \in \mathbb{R}^n$, where bounds on this neighbourhood can be obtained from bounds on $\Delta\mathcal{F}_k$.

Proof: The proof of this result begins by showing that if

$$e_{k+1}^{\mathcal{F}} = \mathcal{D}(e_k^{\mathcal{F}})e_k^{\mathcal{F}}, \tag{23}$$

where $\mathcal{D}(e_k^{\mathcal{F}})$ is as defined by Equation (22), then $e_k^{\mathcal{F}}$ converges to zero in a finite-time stable (FTS) manner. This can be shown by defining the discrete-time Lyapunov function

$$V_k^{\mathcal{F}} := (e_k^{\mathcal{F}})^{\mathrm{T}} e_k^{\mathcal{F}}. \tag{24}$$

Taking the discrete-time difference of this Lyapunov function, we get

$$\begin{aligned} V_{k+1}^{\mathcal{F}} - V_k^{\mathcal{F}} &= -\gamma_k^{\mathcal{F}} (V_k^{\mathcal{F}})^{1/r} \\ \text{where } \gamma_k^{\mathcal{F}} &= (1 - (\mathcal{D}(e_k^{\mathcal{F}}))^2)(V_k^{\mathcal{F}})^{(1-1/r)}. \end{aligned} \tag{25}$$

Note that $\mathcal{D}(e_k^{\mathcal{F}})$ is a monotonically decreasing function of $\|e_k^{\mathcal{F}}\| \in \mathbb{R}_0^+$, taking values in the range $[-1, 1)$, so $\gamma_k^{\mathcal{F}}$ is a positive definite function of $V_k^{\mathcal{F}} = \|e_k^{\mathcal{F}}\|^2$. Substituting $(e_k^{\mathcal{F}})^{\mathrm{T}} e_k^{\mathcal{F}} = V_k^{\mathcal{F}}$ into the expression for $\mathcal{D}(e_k^{\mathcal{F}})$ to evaluate $\gamma_k^{\mathcal{F}}$ in Equation (25), we express $\gamma_k^{\mathcal{F}}$ as a function of $V_k^{\mathcal{F}}$:

$$\gamma_k^{\mathcal{F}} = 4\lambda \frac{(V_k^{\mathcal{F}})^{2-2/r}}{((V_k^{\mathcal{F}})^{1-1/r} + \lambda)^2}. \tag{26}$$

Clearly, Equation (26) shows that $\gamma_k^{\mathcal{F}} := \gamma(V_k^{\mathcal{F}})$ is a class-$\mathcal{K}$ function of $V_k^{\mathcal{F}}$. Further, it can be verified that

$$V_N^{\mathcal{F}} \le \lambda^{\frac{1}{1-1/r}} \iff \gamma_N^{\mathcal{F}} \le \lambda.$$

These two facts together allow as to conclude that this $\gamma_k^{\mathcal{F}}$ (taking the role of γ_k in Lemma 2.1) satisfies the sufficient condition (7) for finite-time stability of $e_k^{\mathcal{F}}$, with a value of $\epsilon = \lambda^{\frac{1}{1-1/r}}$. Using the definition of $e_k^{\mathcal{F}}$ given by Equation (20) and the relation (23), one obtains the following discrete time observer for $\hat{\mathcal{F}}_k$:

$$\hat{\mathcal{F}}_{k+1} = \mathcal{D}(e_k^{\mathcal{F}}) e_k^{\mathcal{F}} + \mathcal{F}_{k+1}. \tag{27}$$

The above expression leads to a finite-time stable observer for the unknown dynamics (uncertain input) $\mathcal{F}_k$ that ensures that the estimation error $e_k^{\mathcal{F}}$ converges to zero for $k > N$ where $N \in \mathbb{W}$ is finite.

However, as mentioned earlier, $\mathcal{F}_{k+1}$ is not available at time t_{k+1} due to causality; therefore, it needs to be replaced by a known quantity. This first-order observer design given by Equation (22) replaces $\mathcal{F}_{k+1}$ in Equation (27) with $\mathcal{F}_k = y_{k+\nu} - \mathcal{G}_k u_k$, which is known from the measured output and applied input from the previous sampling instant. As a result, the estimation error $e_k^{\mathcal{F}}$ evolves according to

$$\begin{aligned} e_{k+1}^{\mathcal{F}} &:= \hat{\mathcal{F}}_{k+1} - \mathcal{F}_{k+1} = \mathcal{D}(e_k^{\mathcal{F}}) e_k^{\mathcal{F}} + \mathcal{F}_k - \mathcal{F}_{k+1} \\ &= \mathcal{D}(e_k^{\mathcal{F}}) e_k^{\mathcal{F}} - \Delta\mathcal{F}_k, \quad \text{where } \Delta\mathcal{F}_k = \mathcal{F}_{k+1} - \mathcal{F}_k. \end{aligned} \tag{28}$$

Therefore, this observer is a first-order perturbation of the ideal FTS observer design for $\mathcal{F}_k$ as given by Equation (27), with the perturbation coming from the first-order difference term $\Delta\mathcal{F}_k$. Due to the FTS behaviour of this ideal observer for $\mathcal{F}_k$, the first-order observer design of Equation (22) will converge to a neighbourhood of $e_k^{\mathcal{F}} = 0$ for finite k, where the size of this neighbourhood depends on bounds on $\Delta\mathcal{F}_k$. As $\mathcal{F}_k$ is Lipschitz continuous, so $\|\Delta\mathcal{F}_k\|$ is bounded according to the first of Equations (19). Clearly, the smaller the bounds on $\Delta\mathcal{F}_k$, the smaller the neighbourhood of $e_k^{\mathcal{F}} = 0$ that this observer will converge to within finite time. ■

In the following result, the observer given by Equation (22) is analytically shown to be robust to known bounds on the norm of the first difference $\Delta\mathcal{F}_k$ in the unknown $\mathcal{F}_k$.

Theorem 3.2: *Consider the observer law* (22) *for the unknown* $\mathcal{F}_k$ *in the ultra-local model* (17) *modelling the unknown system* (3). *Let the first order difference* $\Delta\mathcal{F}_k$ *defined by* (21) *be bounded according to*

$$\|\Delta\mathcal{F}_k\| \le B^{\mathcal{F}}, \tag{29}$$

where $B^{\mathcal{F}} \in \mathbb{R}^+$ *is a known constant. Then the observer (estimation) error* $e_k^{\mathcal{F}}$ *is guaranteed to converge to the neighbourhood given by*

$$\mathcal{N}^{\mathcal{F}} := \{e_k^{\mathcal{F}} \in \mathbb{R}^n : \rho(e_k^{\mathcal{F}})\|e_k^{\mathcal{F}}\| \le B^{\mathcal{F}}\} \tag{30}$$

for finite $k > N$, $N \in \mathbb{W}$, *where*

$$\begin{aligned} \rho(e_k^{\mathcal{F}}) &:= \frac{\zeta(e_k^{\mathcal{F}})}{1 - \sqrt{1 - \zeta(e_k^{\mathcal{F}})}} \\ \text{and} \quad \zeta(e_k^{\mathcal{F}}) &:= 1 - (\mathcal{D}(e_k^{\mathcal{F}}))^2 = \frac{\gamma_k^{\mathcal{F}}}{((e_k^{\mathcal{F}})^{\mathrm{T}} e_k^{\mathcal{F}})^{1-1/r}}. \end{aligned} \tag{31}$$

Proof: Using the Lyapunov function defined by Equation (24) and the observer Equation (22), we obtain

$$\begin{aligned} V_{k+1}^{\mathcal{F}} - V_k^{\mathcal{F}} &= (e_{k+1}^{\mathcal{F}} + e_k^{\mathcal{F}})^{\mathrm{T}} (e_{k+1}^{\mathcal{F}} - e_k^{\mathcal{F}}) \\ &= ((\mathcal{D}(e_k^{\mathcal{F}}))^2 - 1)(e_k^{\mathcal{F}})^{\mathrm{T}} e_k^{\mathcal{F}} - 2\mathcal{D}(e_k^{\mathcal{F}})\Delta F_k^{\mathrm{T}} e_k^{\mathcal{F}} \\ &\quad + \Delta F_k^{\mathrm{T}} \Delta F_k. \end{aligned}$$

Taking into account the bound (29) and the expression for $\gamma_k^{\mathcal{F}}$ given by Equation (25), we get an upper bound on the first difference of this Lyapunov function as follows:

$$\begin{aligned} V_{k+1}^{\mathcal{F}} - V_k^{\mathcal{F}} &\le -\gamma_k^{\mathcal{F}} (V_k^{\mathcal{F}})^{1/r} + 2|\mathcal{D}(e_k^{\mathcal{F}})| B^{\mathcal{F}} \|e_k^{\mathcal{F}}\| + (B^{\mathcal{F}})^2 \\ &= -\zeta(e_k^{\mathcal{F}})\|e_k^{\mathcal{F}}\|^2 + 2|\mathcal{D}(e_k^{\mathcal{F}})| B^{\mathcal{F}} \|e_k^{\mathcal{F}}\| + (B^{\mathcal{F}})^2, \end{aligned} \tag{32}$$

using the definition of the Lyapunov function (24) and Equation (31) for $\zeta(e_k^{\mathcal{F}})$ in the last step. For large enough initial (transient) $\|e_k^{\mathcal{F}}\|$, the right-hand side of the inequality (32) is negative, and we get

$$\zeta(e_k^{\mathcal{F}})\|e_k^{\mathcal{F}}\|^2 + 2|\mathcal{D}(e_k^{\mathcal{F}})| B^{\mathcal{F}} \|e_k^{\mathcal{F}}\| - (B^{\mathcal{F}})^2 > 0,$$

which can be solved as a quadratic inequality expression in $\|e_k^{\mathcal{F}}\|$ with coefficients that depend on $e_k^{\mathcal{F}}$. Noting that $\zeta(e_k^{\mathcal{F}}) = 1 - (\mathcal{D}(e_k^{\mathcal{F}}))^2$, this leads to the condition

$$\zeta(e_k^{\mathcal{F}})\|e_k^{\mathcal{F}}\| > B^{\mathcal{F}}[1 - \sqrt{1 - \zeta(e_k^{\mathcal{F}})}], \tag{33}$$

for real positive solutions of $\|e_k^{\mathcal{F}}\|$ for which $V_{k+1}^{\mathcal{F}} - V_k^{\mathcal{F}} < 0$ is guaranteed. The discrete Lyapunov function $V_k^{\mathcal{F}}$ is monotonically decreasing for such $\|e_k^{\mathcal{F}}\|$ large enough to satisfy inequality (33), which it will until a finite value of k, say $k = N$. Therefore, the observer error $e_k^{\mathcal{F}}$ is guaranteed to converge to the neighbourhood $\mathcal{N}^{\mathcal{F}}$ of $0 \in \mathbb{R}^n$ given by Equations (30)–(31) and will remain in this neighbourhood (which is positively invariant) for $k > N$. ■

Remark 3.1: This first-order observer can become unstable if $\Delta\mathcal{F}_k$ escapes (becomes unbounded) in finite time at a rate faster than that dictated by the design of $\mathcal{D}(e_k^{\mathcal{F}})$. However, the Lipschitz continuity condition imposed by Equations (19) ensures that this cannot happen. The Hölder continuity of the feedback system, as given by Theorem 2.1, guarantees robustness to Lipschitz continuous uncertainties according to Theorem 3.2.

Remark 3.2: Note that the bound on $\|e_k^{\mathcal{F}}\|$ given by the sufficient condition in Theorem 3.2 is conservative. Moreover, as $\Delta\mathcal{F}_k$ is bounded according to the Lipschitz condition (19), the bound on it given by (29) is already likely to be conservative for small changes in states between successive output measurements. Therefore, this sufficient condition is conservative.

3.3 Estimation of unknown input–output dynamics using a second order Observer

In this subsection, we design a second order observer for $\mathcal{F}_k$ based on the developments in the previous subsection. To start the design process, we reverse Equation (21) to obtain

$$\mathcal{F}_{k+1} = \mathcal{F}_k + \Delta\mathcal{F}_k. \tag{34}$$

The second-order observer design is based on the above expression, as follows:

$$\hat{\mathcal{F}}_{k+1} = \hat{\mathcal{F}}_k + \Delta\hat{\mathcal{F}}_k, \tag{35}$$

where $\Delta\hat{\mathcal{F}}_k$ is the estimate of $\Delta\mathcal{F}_k$. In addition, define the error in estimating $\Delta\mathcal{F}_k$ as follows:

$$e_k^{\Delta} := \Delta\hat{\mathcal{F}}_k - \Delta\mathcal{F}_k. \tag{36}$$

The following result gives the second order observer designed to estimate $\mathcal{F}_k$ and $\Delta\mathcal{F}_k$.

Theorem 3.3: *Let e_k^{Δ} be as defined by Equation* (36)*, and $e_k^{\mathcal{F}}$, $r \in]1, 2[$ and $\lambda > 0$ be as defined in Theorem* 3.1*. Further, let $\mathcal{D}(\cdot)$ be as defined by Equation* (22) *in Theorem* 3.1*, and let the second order finite-time difference given by*

$$\Delta^2\mathcal{F}_k := \mathcal{F}_{k-1}^{(2)} = \mathcal{F}_{k+1} - 2\mathcal{F}_k + \mathcal{F}_{k-1} \tag{37}$$

be bounded as obtained from the first of Equations (19)*. Let the control influence matrix $\mathcal{G}_k$ be designed such that its first-order finite difference is bounded as in the second of Equations* (19)*. Consider the nonlinear observer given by*

$$\hat{\mathcal{F}}_{k+1} = \mathcal{D}(e_k^{\mathcal{F}})e_k^{\mathcal{F}} + \mathcal{F}_k + \Delta\hat{\mathcal{F}}_k \text{ given } \hat{\mathcal{F}}_0,$$
$$\text{where } \Delta\hat{\mathcal{F}}_k = \mathcal{D}(e_{k-1}^{\Delta})e_{k-1}^{\Delta} + \Delta\mathcal{F}_{k-1}, \tag{38}$$

and $\mathcal{F}_k = y_{k+\nu} - \mathcal{G}_k u_k$ according to the ultra-local model (17)*. This observer leads to finite time stable convergence of the estimation errors $(e_k^{\mathcal{F}}, e_k^{\Delta}) \in \mathbb{R}^n \times \mathbb{R}^n$ to bounded neighbourhoods of $(0, 0) \in \mathbb{R}^n \times \mathbb{R}^n$, where these bounds can be obtained from bounds on $\Delta^2\mathcal{F}_k$.*

Proof: The proof of this result starts by noting that the ideal FTS observer law for $\mathcal{F}_k$ given by Equation (27) can also be expressed as

$$\hat{\mathcal{F}}_{k+1} = \mathcal{D}(e_k^{\mathcal{F}})e_k^{\mathcal{F}} + \mathcal{F}_k + \Delta\mathcal{F}_k, \tag{39}$$

because the last two terms on the right-hand side of this expression add up to $\mathcal{F}_{k+1}$. The second-order observer law given by Equation (38) is obtained by replacing $\Delta\mathcal{F}_k$ on the RHS of Equation (39) with its estimate. The estimate $\Delta\hat{\mathcal{F}}_k$ would converge to the true value $\Delta\mathcal{F}_k$ in finite time, if it is updated according to the (ideal) observer law

$$\Delta\hat{\mathcal{F}}_k = \mathcal{D}(e_{k-1}^{\Delta})e_{k-1}^{\Delta} + \Delta\mathcal{F}_k. \tag{40}$$

Note that this ideal observer for $\Delta\mathcal{F}_k$ is of the same form as the ideal FTS observer law for $\mathcal{F}_k$ given by Equation (27). Further, like the ideal observer (27), the observer Equation (40) is not practically implementable because $\Delta\mathcal{F}_k$ is unknown at time t_k (because $\mathcal{F}_{k+1}$ is unknown). As we did with the first order observer in Theorem 3.1, we replace $\Delta\mathcal{F}_k$ in (40) with its previous value, assuming that the change in this quantity is small in the time interval $[t_{k-1}, t_k]$. This leads to the following observer law for $\Delta\mathcal{F}_k$:

$$\Delta\hat{\mathcal{F}}_k = \mathcal{D}(e_{k-1}^{\Delta})e_{k-1}^{\Delta} + \Delta\mathcal{F}_{k-1}. \tag{41}$$

The resulting second-order observer is therefore given by Equations (38). To show that this is indeed second order, the evolution of the estimation error $e_k^{\mathcal{F}}$ in discrete time is obtained as below

$$\begin{aligned} e_{k+1}^{\mathcal{F}} &:= \hat{\mathcal{F}}_{k+1} - \mathcal{F}_{k+1} = \mathcal{D}(e_k^{\mathcal{F}})e_k^{\mathcal{F}} + \mathcal{D}(e_{k-1}^{\Delta})e_{k-1}^{\Delta} \\ &\quad + \mathcal{F}_k + \Delta\mathcal{F}_{k-1} - \mathcal{F}_{k+1} \\ &= \mathcal{D}(e_k^{\mathcal{F}})e_k^{\mathcal{F}} + \mathcal{D}(e_{k-1}^{\Delta})e_{k-1}^{\Delta} - \Delta^2\mathcal{F}_k, \end{aligned} \tag{42}$$

where $\Delta^2\mathcal{F}_k$ is as defined by Equation (37). The last line in the above expression is obtained by substituting for $\Delta\mathcal{F}_{k-1}$ in the previous line, using the definition of $\Delta\mathcal{F}_k$ given by Equation (21). The remainder of the proof of this result uses the same arguments as in the last part of the proof of Theorem 3.1, with $\Delta\mathcal{F}_k$ replaced by $\Delta^2\mathcal{F}_k$ and $\Delta\mathcal{F}_k$, $\Delta\mathcal{G}_k$ bounded as in Equations (19). ■

Remark 3.3: Sufficient conditions on the bounds on neighbourhoods of $0 \in \mathbb{R}^n$ that the estimation errors $e_k^{\mathcal{F}}, e_k^{\Delta} \in \mathbb{R}^n$ converge to for the observer in Theorem 3.3 can be obtained in a manner similar to the bounds given by Theorem 3.2 for the estimation error obtained from the observer in Theorem 3.1.

Remark 3.4: It is clear from the constructive proofs of Theorems 3.1 and 3.3 that higher-order observers for $\mathcal{F}_k$ may be constructed using a similar process. For example, a third-order observer can be constructed by replacing $\Delta\mathcal{F}_{k-1}$ in the second line of Equation (38) with $\Delta\mathcal{F}_{k-1} + \Delta^2\hat{\mathcal{F}}_{k-1}$ and finding an appropriate update law for $\Delta^2\hat{\mathcal{F}}_{k-1}$. Clearly, the added computational burden of higher-order observers makes them unattractive for implementation when the higher-order differences of the discrete signal $\mathcal{F}_k$ are known to be within reasonable bounds. In most situations, the uncertainty $\mathcal{F}_k$ is Lipschitz continuous as given by Equation (19), and bounds on $\Delta\mathcal{F}_k$ and $\Delta^2\mathcal{F}_k$ can be obtained; therefore, these low order observers are adequate.

Remark 3.5: Note that both the observers given by Theorems 3.1 and 3.3 provide *exact* finite-time stable convergence of estimation errors $e_k^{\mathcal{F}}$ (and e_k^{Δ} for Theorem 3.3) to zero if $\mathcal{F}_k$ is constant. Therefore, the resulting feedback loop with either of these uncertainty observers rejects constant unknown input signals $\mathcal{F}_k$.

4. Model-free nonlinearly stable feedback tracking control

In this section, we design tracking control laws for the control input u_k from the output y_k, the desired output y_k^d, and the estimate of the ultra-local model $\hat{\mathcal{F}}_k$ constructed from output measurement y_k and past input–output history as described in Section 3. This section provides two nonlinear model-free output feedback tracking control schemes that solve Problem 3.1 in Section 3.1. The control design process is based on Assumptions 2.1, 2.2 and 2.3 for the discrete nonlinear system (2), and is designed to track a desired output trajectory for a system expressed by the ultra-local model (17). The control designs given here may make use of either of the nonlinear observers for the ultra-local model given in Sections 3.2 and 3.3, but is independent of these observers designed in the previous section. They can be used in conjunction with other uncertainty (or ultra-local model) observers that do the same task.

4.1 *First output trajectory tracking control law*

Let $y^d : \mathbb{R} \to \mathbb{R}^n$ be a C^ν function that gives a desired output trajectory that is ν times differentiable according to Assumption 2.3, and denote $y_k^d := y^d(t_k)$ for $\{t_k\} \subset \mathbb{R}_0^+$. Considering Problem 3.1, define the output trajectory tracking error

$$e_k^y = y_k - y_k^d \quad \text{where } y_k^d = y^d(t_k). \tag{43}$$

The first control law design presented here has the following objectives: (1) to ensure that the feedback system tracks the desired trajectory in a nonlinearly stable manner; and (2) to ensure that the tracking error is ultimately bounded by the same ultimate bounds that bound the observer error in the model estimate, $e_k^{\mathcal{F}}$.

Proposition 4.1: *Consider an unknown input–output system described by the ultra-local model* (17) *with the control law*

$$\mathcal{G}_k u_k = y_{k+\nu}^d - \hat{\mathcal{F}}_k, \tag{44}$$

where the $y_i^d = y^d(t_i)$ describe a desired output trajectory for the time sequence $\{t_i\} \subset \mathbb{R}_0^+$ as in Equation (43)*. The trajectory tracking error e_k^y defined by* (43) *then satisfies*

$$e_{k+\nu}^y + e_k^{\mathcal{F}} = 0, \tag{45}$$

where $e_k^{\mathcal{F}}$ is the model estimation error defined by (20)*. In particular, if the model estimate $\hat{\mathcal{F}}_k$ is given by the observer in Theorems* 3.1 *or* 3.3*, then $e_{k+\nu}^y$ converges to a bounded neighbourhood of $0 \in \mathbb{R}^n$ in finite time (for finite k), where the bounds on this neighbourhood are given by the same bounds that bound the estimation error $e_k^{\mathcal{F}}$.*

Proof: The short proof starts by noting that

$$y_{k+\nu} - y_{k+\nu}^d = \mathcal{F}_k + \mathcal{G}_k u_k - y_{k+\nu}^d. \tag{46}$$

Now define

$$w_k := \mathcal{G}_k u_k + \hat{\mathcal{F}}_k. \tag{47}$$

Substituting for $\mathcal{G}_k u_k$ from Equation (47) into Equation (46), we obtain

$$e_{k+\nu}^y = \mathcal{F}_k + w_k - \hat{\mathcal{F}}_k - y_{k+\nu}^d = w_k - e_k^{\mathcal{F}} - y_{k+\nu}^d. \tag{48}$$

After substituting the control law Equation (44) into expression (48) and collecting terms, we get Equation (45). ■

An immediate corollary of this result follows.

Corollary 4.1: *If the uncertainty modelled by $\mathcal{F}_k$ in the ultra-local model* (17) *is constant, then the control law* (44) *along with the observer* (22) *or* (38)*, lead to stable finite-time convergence of tracking error e_k^y to zero.*

This follows immediately from Remark 3.5 about the uncertainty (ultra-local model) observers given in Section 3, and Proposition 4.1. Although the control law (44) is simple to implement, note that it does not include direct feedback of the output tracking error, e_k^y. This may lead to a lack of robustness to errors in measuring the output signal y_k. The following subsection gives another control law that does not have this drawback and is robust to output measurement errors.

4.2 *Second output trajectory tracking control law*

The second tracking control law follows from:

$$y_{k+\nu} = \hat{\mathcal{F}}_k + \mathcal{G}_k u_k \quad \text{if } e_k^{\mathcal{F}} = 0. \tag{49}$$

In this case, the output tracking error satisfies

$$e_{k+\nu}^y = \hat{\mathcal{F}}_k + \mathcal{G}_k u_k - y_{k+\nu}^d. \tag{50}$$

The statement below gives a tracking control law that includes feedback of the output tracking error.

Theorem 4.1: *Consider an unknown input–output system described by the ultra-local model* (17)*. Let e_k^y be as defined by Equation* (43)*, and let $s \in]1, 2[$ and $\mu \in \mathbb{R}^+$ be constants. Let the control law for the system be given by*

$$\mathcal{G}_k u_k = y_{k+\nu}^d - \hat{\mathcal{F}}_k + \mathcal{C}(e_{k+\nu-1}^y) e_{k+\nu-1}^y, \\ \text{where } \mathcal{C}(e_j^y) = \frac{((e_j^y)^{\mathrm{T}} e_j^y)^{1-1/s} - \mu}{((e_j^y)^{\mathrm{T}} e_j^y)^{1-1/s} + \mu}, \tag{51}$$

and the $y^d_j = y^d(t_j)$ describe a desired output trajectory for the time sequence $\{t_i\} \subset \mathbb{R}^+_0$ as in Equation (43)*. Then the system* (17) *with the unknown dynamics $\mathcal{F}^k$ along with the control law* (51)*, satisfies the error dynamics*

$$e^y_{k+\nu} + e^{\mathcal{F}}_k = \mathcal{C}(e^y_{k+\nu-1})e^y_{k+\nu-1}. \tag{52}$$

In particular, if the uncertainty estimate $\hat{\mathcal{F}}^k$ is obtained from the observer law (22) *of Theorem* 3.1 *or* (38) *of Theorem* 3.3*, then $e^y_{k+\nu}$ converges in a stable manner to a bounded neighbourhood of* $0 \in \mathbb{R}^n$ *after finite time* (*i.e. for finite $k \in \mathbb{W}$*)*.*

Proof: We begin the proof of this result by noting that if $e^{\mathcal{F}}_k = 0$, then $e^y_{k+\nu}$ satisfies Equation (50). In this situation, the estimation of $\mathcal{F}_k$ is perfect, and finite-time stable convergence of the output tracking error to zero is guaranteed if

$$e^y_{k+\nu} = \mathcal{C}(e^y_{k+\nu-1})e^y_{k+\nu-1}, \tag{53}$$

with $\mathcal{C}(e^y_j)$ defined as in Equation (51). Note that the design of $\mathcal{C}(e^y_j)$ is similar to the design of $\mathcal{D}(e^{\mathcal{F}}_k)$ in the observer law (22). Defining the following Lyapunov function for the output tracking error:

$$V^y_k := (e^y_k)^{\mathrm{T}} e^y_k, \tag{54}$$

we can easily show that the error dynamics (53) leads to finite-time stable convergence of the output tracking error e^y_k to zero; this would parallel the stability analysis in Theorem 3.1 for the model (uncertainty) estimation error $e^{\mathcal{F}}_k$. Based on Corollary 4.1, we know that perfect estimation of $\mathcal{F}_k$ happens when $\mathcal{F}_k$ is constant, for example; this is one case where $e^{\mathcal{F}}_k = 0$ for $k > N$ and a finite $N \in \mathbb{W}$. In all such situations, Equation (53) ensures convergence of the output tracking error e^y_k to zero in (an additional) finite amount of time.

More generally, if $e^{\mathcal{F}}_k$ reaches a bounded neighbourhood of the zero vector in $\mathbb{R}^n$, as would be the case if the observer laws given by either (22) of Theorem 3.1 or (38) of Theorem 3.3 are used, then the control law (51) leads to the following feedback dynamics:

$$y_{k+\nu} = y^d_{k+\nu} - e^{\mathcal{F}}_k + \mathcal{C}(e^y_{k+\nu-1})e^y_{k+\nu-1}, \tag{55}$$

when substituted into the ultra-local model (17). Re-arranging terms in Equation (55), we get the error dynamics (52). Note that the error dynamics (52) is a perturbation of the finite-time stable tracking error dynamics given by (53), where the perturbation is due to the bounded error $e^{\mathcal{F}}_k$ in estimating the unknown dynamics. ■

In the following subsection, we provide results on the robustness of this trajectory tracking control law in the presence of bounded estimation error $e^{\mathcal{F}}_k$ in estimating the unknown dynamics $\mathcal{F}_k$ and bounded measurement error (noise) η_k in the measured outputs y_k.

4.3 Robustness of second output tracking control scheme

The convergence of the output tracking error e^y_k to zero for the control laws (44) in Proposition 4.1 and (51) in Theorem 4.1, is contingent upon $e^{\mathcal{F}}_k$ converging to zero in finite time, which happens in the special case that $\mathcal{F}_k$ is constant according to Corollary 4.1. However, the usefulness of this control law (51) is its robustness to errors in the estimation of $\mathcal{F}_k$, as given by the following result.

Proposition 4.2: *Consider the feedback system consisting of the unknown system given by the ultra-local model* (17)*, the observer law* (22) *or the observer law* (38)*, and the control law* (51)*. Let the estimation error $e^{\mathcal{F}}_k$ in the unknown $\mathcal{F}_k$ be bounded according to*

$$\|e^{\mathcal{F}}_k\| \le B \quad \textit{for } k > N, \tag{56}$$

where $B \in \mathbb{R}^+$ and $N \in \mathbb{W}$ are known. Then the tracking error e^y_k converges to the neighbourhood given by

$$\mathcal{N}^y := \{e^y_k \in \mathbb{R}^n : \sigma(e^y_k)\|e^y_k\| \le B\}, \tag{57}$$

for $k > N' > N$, $N' \in \mathbb{W}$, where

$$\sigma(e^y_k) := \frac{\beta(e^y_k)}{1 - \sqrt{1 - \beta(e^y_k)}}, \quad \beta(e^y_k) := 1 - (\mathcal{C}(e^y_k))^2. \tag{58}$$

Proof: The proof of this result is similar to the proof of Theorem 3.2. The feedback tracking error e^y_k satisfies Equation (52). The first difference of the Lyapunov function (54) is evaluated as follows:

$$\begin{aligned} V^y_{k+1} - V^y_k &= (e^y_{k+1} + e^y_k)^{\mathrm{T}}(e^y_{k+1} - e^y_k) \\ &= ((\mathcal{C}(e^y_k))^2 - 1)(e^y_k)^{\mathrm{T}} e^y_k - 2\mathcal{C}(e^y_k)(e^{\mathcal{F}}_k)^{\mathrm{T}} e^y_k + (e^{\mathcal{F}}_k)^{\mathrm{T}} e^{\mathcal{F}}_k. \end{aligned}$$

With the bound on $e^{\mathcal{F}}_k$ given by (56) for $k > N$, we get an upper bound on the first difference of this Lyapunov function as follows:

$$V^y_{k+1} - V^y_k \le -\beta(e^y_k)\|e^y_k\|^2 + 2|\mathcal{C}(e^y_k)|B\|e^y_k\| + B^2, \tag{59}$$

using the expression for V^y_k in Equations (54) and (58) for $\beta(e^y_k)$. The remainder of this proof follows the same last few steps as the proof of Theorem 3.2, with the appropriate substitutions, i.e. $e^{\mathcal{F}}_k$ replaced by e^y_k, $\mathcal{D}(e^{\mathcal{F}}_k)$ by $\mathcal{C}(e^y_k)$, $B^{\mathcal{F}}$ by B, and $\zeta(e^{\mathcal{F}}_k)$ by $\beta(e^y_k)$. This leads to the conclusion that for $k > N'$ for some whole number $N' > N$, the tracking error e^y_k converges to the neighbourhood of the origin in $\mathbb{R}^n$ given by Equations (57)–(58). ■

In the presence of output measurement errors, an output observer can be implemented that filters out measurement noise and gives output estimates. The above result can then be extended to show robustness to both output estimation errors and model (uncertainty) estimation errors in this situation, as a result below shows.

Corollary 4.2: *Consider the feedback system consisting of the unknown system given by* (17)*, with output measurements corrupted by bounded noise $\eta_k \in \mathbb{R}^n$ as given by* (6)*. Let a stable output observer provide output estimates $\hat{y}_k$ with bounded estimation errors $e^o_k := \hat{y}_k - y_k$. Consider the feedback tracking control law Equation* (51) *with the 'observed' tracking error now* *defined as* $\hat{e}^y_k := \hat{y}_k - y^d_k$, *used in conjunction with either of the ultra-local model (uncertainty) observers given by Equations* (22) *or* (38). *Then the resulting feedback system is (Lyapunov) stable and robust to errors in the ultra-local model estimate* $e^{\mathcal{F}}_k$ *and the bounded observer error* e^o_k. *Further, if* $e^{\mathcal{F}}_k$ *is bounded according to* (56), *then the observed tracking error* $\hat{e}^y_k$ *converges to a neighbourhood of the form* $\hat{\mathcal{N}}^y$ *where*

$$\hat{\mathcal{N}}^y := \{\hat{e}^y_k \in \mathbb{R}^n \, : \, \sigma(\hat{e}^y_k)\|\hat{e}^y_k\| \le B\}, \tag{60}$$

for $k > N' > N$, $N' \in \mathbb{W}$, *where* $\sigma(\cdot)$ *is as defined by* (58) *and* N *is according to* (56).

Proof: The proof of this result is identical to that of Proposition 4.2, with the substitution of the feedback control law (51) in terms of $\hat{e}^y_k$:

$$\mathcal{G}_k u_k = y^d_{k+\nu} - \hat{\mathcal{F}}_k + \mathcal{C}(\hat{e}^y_{k+\nu-1})\hat{e}^y_{k+\nu-1}, \tag{61}$$

into the ultra-local model (ULM) given by Equation (17). ■

In the next section, we numerically apply this control scheme with the first-order ULM observer in Section 3.2.

5. Numerical simulation results

Here, we provide numerical simulation results of this model-free tracking control framework applied to an inverted pendulum on a cart with nonlinear friction terms affecting the motion of both degrees of freedom. The dynamics model of this system, unknown to the controller, is described in Section 5.1. The numerical results of the control scheme are given in Section 5.3.

5.1 Inverted pendulum on cart system

The inverted pendulum on the cart is a two-degree-of-freedom mechanical system, with the cart position x considered positive to the right of a fixed origin and the angular displacement θ considered positive counter-clockwise from upward vertical, as shown in Figure 1. The inputs to the system are a horizontal force on the cart denoted F and a torque applied to the pendulum motor where it is attached to the cart denoted τ. The outputs are the cart position x and the angular displacement of the pendulum θ. Therefore, this is a two-input and two-output system, unlike the usual single-input inverted pendulum on a cart example considered with only the horizontal cart force as an input. The mass and rotational inertia of the pendulum are m and I respectively, its length is $2l$, and the mass of the cart is M. A dynamics model of the system, which is unknown for the purpose of control design, is used to generate the desired output trajectory to be tracked. Then the model-free control scheme is used to track this desired trajectory.

For simulation purposes, the inverted pendulum on a cart system is subjected to a nonlinear friction force acting on the cart's motion, and a nonlinear friction-induced torque acting on the pendulum. The friction force acting on the cart is denoted F_x and the friction torque acting on the pendulum is denoted

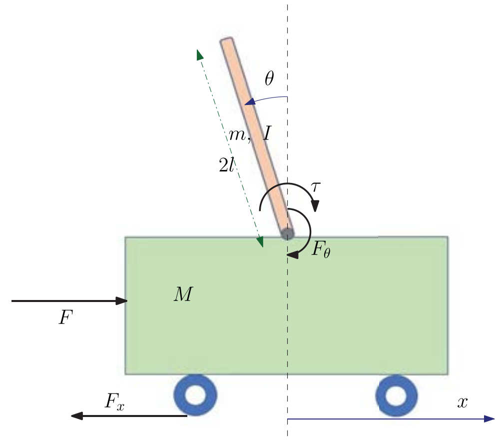

Figure 1. Inverted pendulum system to which our nonlinear model-free control framework is applied.

F_θ, and they are given by

$$F_x = c_x \tanh \dot{x}, \quad F_\theta = c_\theta \tanh \dot{\theta}. \tag{62}$$

Note that the hyperbolic tangent function ensures that these frictional effects get saturated at high speeds ($\dot{x}$ and $\dot{\theta}$). Therefore, the dynamics model of this system, which is unknown for the purpose of control design, is given by

$$\begin{aligned} &\mathcal{M}(q)\ddot{q} + \mathcal{D}(q,\dot{q}) = u, \quad q = \begin{bmatrix} x \\ \theta \end{bmatrix}, \\ &\mathcal{M}(q) = \begin{bmatrix} M+m & -ml\cos\theta \\ -ml\cos\theta & I+ml^2 \end{bmatrix}, \\ &\mathcal{D}(q,\dot{q}) = \begin{bmatrix} ml\dot{\theta}^2\sin\theta + c_x\tanh\dot{x} \\ c_\theta\tanh\dot{\theta} - mgl\sin\theta \end{bmatrix}. \end{aligned} \tag{63}$$

The input and output vectors are

$$u = \begin{bmatrix} F \\ \tau \end{bmatrix}, \quad y = q = \begin{bmatrix} x \\ \theta \end{bmatrix}. \tag{64}$$

For the purpose of the numerical simulation, the parameter values selected for this system are

$$\begin{aligned} &M = 1.5\,\text{kg}, \quad m = 0.5\,\text{kg}, \quad l = 1.4\,\text{m}, \quad I = 0.84\,\text{kg}\,\text{m}^2, \\ &g = 9.8\,\text{m/s}^2, \quad c_x = 0.028\,\text{N}, \quad c_\theta = 0.0032\,\text{N}\,\text{m}. \end{aligned} \tag{65}$$

The desired trajectory was generated by applying the following model-based control inputs (force and torque) to the cart and pendulum:

$$\begin{aligned} F &= ml\dot{\theta}^2\sin\theta - 2(M + m\sin^2\theta)g\sin\theta \\ &\quad - (M+m)g\sin\theta, \quad \tau = -mgl\sin\theta. \end{aligned}$$

This generates an output trajectory $y^d(t) = [x^d(t)\,\theta^d(t)]^{\mathrm{T}}$ that is oscillatory, as depicted in Figure 2 in Section 5.3. Note that this dynamics model and model-based control used here is purely for the purpose of trajectory generation and to demonstrate the working of the model-free control framework outlined in this paper.

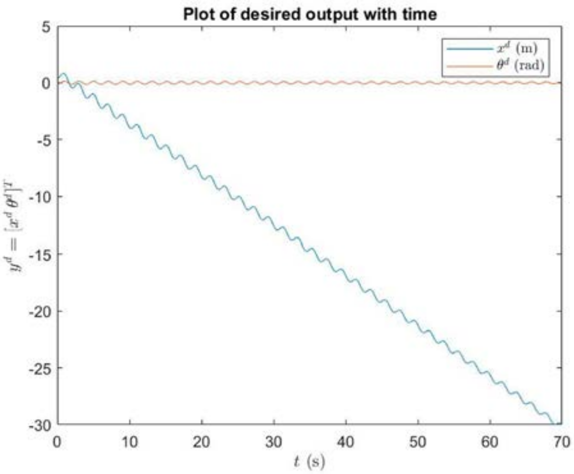

Figure 2. Desired trajectory generated for $T = 70$ seconds for inverted pendulum on cart system.

5.2 Discretisation of continuous dynamics model

The dynamics model and control law for the inverted pendulum on cart system given in Section 5.1, are discretised here using forward difference schemes for generalised velocities and accelerations of the two degrees of freedom. Denoting outputs and inputs in discrete time by $y_k := q_k = q(t_k)$ and $u_k := u(t_k)$ as before and the time step size by $\Delta t := t_{k+1} - t_k$, we get the following discretisation of the continuous dynamics (63)

$$\frac{y_{k+2} - 2y_{k+1} + y_k}{\Delta t^2} = (\mathcal{M}(y_k))^{-1}\left(u_k - \mathcal{D}(y_k, \frac{y_{k+1} - y_k}{\Delta t})\right), \tag{66}$$

where $\mathcal{M}(\cdot)$ and $\mathcal{D}(\cdot,\cdot)$ are as defined in Equation (63). This leads to the following second order discrete-time system:

$$y_{k+2} = \mathsf{F}_k + \mathsf{G}_k u_k, \text{ where } \mathsf{G}_k = \Delta t^2(\mathcal{M}(y_k))^{-1}$$
$$\text{and} \quad \mathsf{F}_k = 2y_{k+1} - y_k - \Delta t^2(\mathcal{M}(y_k))^{-1}\mathcal{D}\left(y_k, \frac{y_{k+1} - y_k}{\Delta t}\right), \tag{67}$$

where F_k and G_k have the meanings as defined by Equation (5). In the numerical simulation results shown in the next subsection, this discrete time system is used for generating the desired output trajectory starting from a given initial state vector and with the control laws given by Equations (66) sampled at time instants t_k. It is then used to simulate the performance of the data-driven control approach outlined in Sections 3 and 4 with the discrete dynamics (67) unknown to the control law.

5.3 Simulation results for control scheme

Here, we present numerical simulation results for the model-free tracking control scheme applied to the system described by Equations (63)–(65). A trajectory is generated for this system using the control scheme (66) sampled in discrete time, with the initial states:

$$\begin{bmatrix} q^d(0) \\ \dot{q}^d(0) \end{bmatrix} = \begin{bmatrix} x^d(0) \\ \theta^d(0) \\ \dot{x}^d(0) \\ \dot{\theta}^d(0) \end{bmatrix} = \begin{bmatrix} 0.45\ \text{m} \\ -0.14\,\text{rad} \\ -0.3\,\text{m/s} \\ 0.05\,\text{rad/s} \end{bmatrix}. \tag{68}$$

The generated trajectory $y^d(t) = \theta^d(t)$ for a time interval of $T = 70$ s is depicted in Figure 2.

The control scheme given by Theorem 4.1 is applied to this system to track this desired trajectory. For this simulation, the initial estimated states are

$$\begin{bmatrix} \hat{q}(0) \\ \dot{\hat{q}}(0) \end{bmatrix} = \begin{bmatrix} \hat{x}(0) \\ \hat{\theta}(0) \\ \dot{\hat{x}}(0) \\ \dot{\hat{\theta}}(0) \end{bmatrix} = \begin{bmatrix} 0\,\text{m} \\ 0.102\,\text{rad} \\ 0\,\text{m/s} \\ 0\,\text{rad/s} \end{bmatrix}. \tag{69}$$

Output measurements are assumed at a constant rate of 100 Hz, i.e.sampling period $\Delta t = 0.01$ s. In the simulation, the measurements are generated by numerically propagating the true discrete-time dynamics of the inverted pendulum on cart system given by Equation (67), and adding noise to the true outputs $y_k = q_k$. The additive noise is generated as high frequency and low amplitude sinusoidal signals, where the frequencies are also sinusoidally time-varying. A finite-time stable output observer given by

$$\hat{y}_{k+1} = y_{k+1} + \mathcal{B}(e_k^o)e_k^o, \text{ where } e_k^o = \hat{y}_k - y_k,$$
$$\text{and} \quad \mathcal{B}(e_k^o) = \frac{((e_k^o)^{\mathrm{T}} L e_k^o)^{1-1/p} - \beta}{((e_k^o)^{\mathrm{T}} L e_k^o)^{1-1/p} + \beta}. \tag{70}$$

with the observer gains

$$L = 2.1, \quad \beta = 2, \quad \text{and} \quad p = \frac{7}{5}, \tag{71}$$

is used to filter out noise from the measured outputs. The first order ultra-local model observer given by Theorem 3.1 is used, with observer gains

$$\lambda = 1.5, \quad \text{and} \quad r = \frac{9}{7}. \tag{72}$$

This observer is initialised with the zero vector, i.e. $\hat{\mathcal{F}}_0 = 0$. The control law (51) is then used to compute the control inputs u_k. The control gains used in this simulation are

$$s = \frac{11}{9}, \quad \mu = 0.35, \quad \text{and} \quad \mathcal{G}_k = \Delta t \begin{bmatrix} 0.559 & 0.196 \\ 0.196 & 0.657 \end{bmatrix}, \tag{73}$$

where $\mathcal{G}_k$ is selected to be symmetric and positive definite based on the expected form for a mechanical system.

Simulation results for the estimation error in estimating the unknown $\mathcal{F}_k$ according to the observer given by Theorem 3.1 in Section 3.2 is depicted in Figure 3. Simulation results for the tracking control performance and control input are shown in Figure 4. The plot on the top shows the output trajectory tracking error over the simulated duration. Note that the tracking error settles down to within an error boundless than about 0.5 m in cart position and 0.05 rad in pendulum angle in steady-state, after an initial brief period of transients. The time plot of the control inputs is shown in the bottom plot. These control input profiles show some high-frequency oscillations in tracking the desired trajectory that seem to correlate with the oscillations seen in the ultra-local model observer error in Figure 3. Future work will deal with reducing these transients by using the

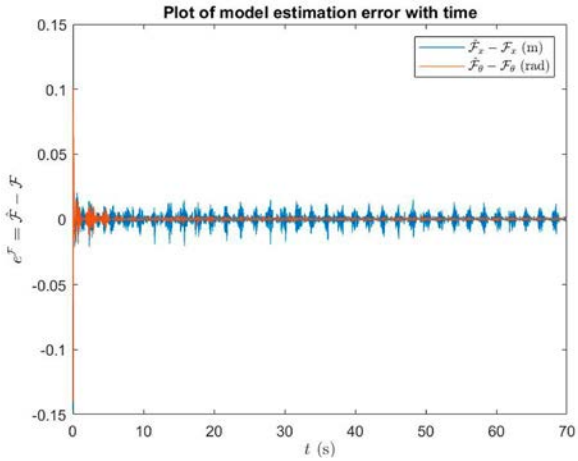

Figure 3. Estimation error in ultra-local model estimation (bottom) for inverted pendulum on cart system with model-free control.

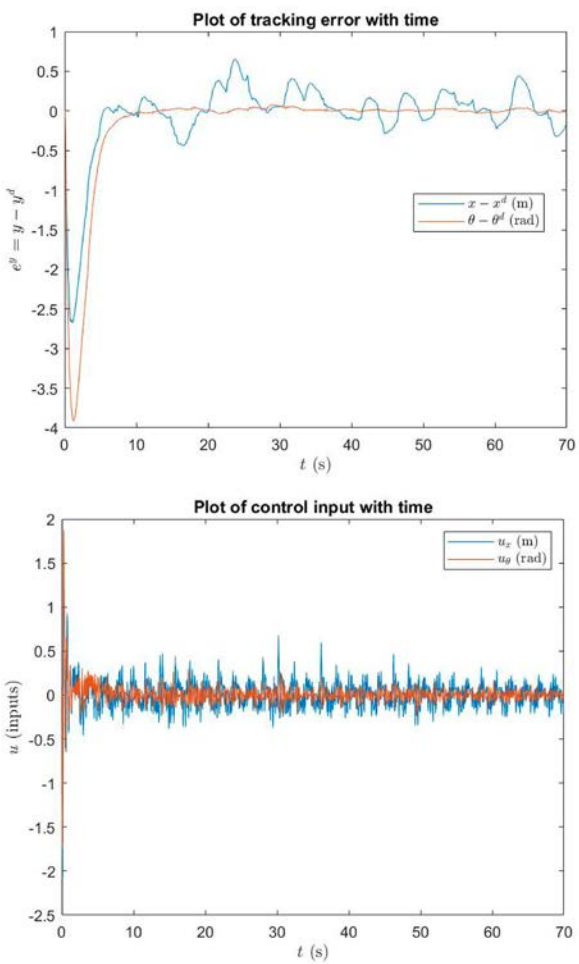

Figure 4. Output trajectory tracking error (top) and control input (bottom) for inverted pendulum on cart system with model-free control.

integral term(s) in the observer designs to produce smoother estimates of the output and ultra-local model. A reference governor may also be used to modify the reference (desired) output trajectory based on current estimates of outputs as in Garone and Nicotra (2016).

Remark 5.1: Although the schemes given here assume that the output space is a vector space, the angle output for this inverted pendulum on cart example is on the circle $\mathbb{S}^1$, which is not a vector space. Therefore, the observer and control laws outlined in the earlier sections may lead to unwinding, even though that does not happen for the numerical simulation reported here. The model-free observer and controller design framework outlined here will be extended to systems evolving on non-Euclidean output (or state) spaces in the future to address this issue.

6. Conclusion

This paper presents a framework for data-driven (model-free) control that guarantees nonlinear stability and robustness for output tracking control with the feedback of output measurements in discrete time. The formulation presented here is developed in discrete time, and uses the concept of an ultra-local model used to model unknown input–output behaviour, similar to the linear model-free control approach formulated in the last decade. This formulation begins with a finite-time stabilisation scheme in discrete-time that leads to a Hölder-continuous feedback system. This finite-time stabilisation scheme is then used to develop nonlinearly stable and robust observers to estimate in real-time the ultra-local model that models the unknown input–output dynamics, from past input–output history. The estimates of the unknown dynamics are then used for compensation of these unknowns (considered as an uncertain input) in a nonlinear output feedback tracking control law that is designed to track a desired output trajectory that is smooth, in a nonlinearly stable and robust manner. Nonlinear stability analysis shows the stability of the feedback compensator combining the nonlinear observer and nonlinear control law when the change in the discrete-time system dynamics modelled by the ultra-local model has a bounded finite difference. A numerical simulation experiment is carried out on an inverted pendulum on a cart system with nonlinear friction, for which the inputs are the horizontal force applied to the cart and a torque applied to the pendulum, and the outputs are the cart horizontal displacement and angular displacement of the pendulum from the upward vertical. The simulation includes bounded noise in measured outputs. The model of the dynamics of this system is unknown to the nonlinear observers and controller designed using our nonlinear model-free control framework. This numerical experiment shows convergence of output estimation errors and output tracking errors to small absolute values. Future work will explore extensions of this framework to systems with constrained control inputs, discrete-time systems with multi-rate inputs and outputs, and systems evolving on Lie groups and their principal bundles. A combined stability analysis that combines the proof of stability of uncertainty estimation as well as output tracking using a single, combined Lyapunov function, may also be explored in the future.

Acknowledgements

The author acknowledges helpful discussions and support from his hosts at the Systems and Control (SysCon) Department at Indian Institute of Technology, Bombay, India, (IIT-B) during the summer of 2019, when commencing this work.

Disclosure statement

No potential conflict of interest was reported by the author(s).

Funding

This work was supported by the National Science Foundation [grant number IIP 1938518].

ORCID

A. K. Sanyal http://orcid.org/0000-0002-3258-7841

References

Bhat, S., & Bernstein, D. (2000). Finite-time stability of continuous autonomous systems. *SIAM Journal on Control and Optimization*, *38*(3), 751–766. https://doi.org/10.1137/S0363012997321358

Bohn, J., & Sanyal, A. K. (2015). Finite time stabilization of simple mechanical systems using continuous feedback. *International Journal of Control*, *88*(4), 783–791. https://doi.org/10.1080/00207179.2014.974675

Chang, C., Duenas, V. H., & Sanyal, A. (2020). *Model free nonlinear control with finite-time estimation applied to closed-loop electrical stimulation induced cycling*. 2020 American Control Conference (ACC), Denver, CO (pp. 5182–5187). IEEE. https://doi.org/10.23919/ACC45564.2020.9147327

Chang, Y., Gao, B., & Gu, K. (2011). A model-free adaptive control to a blood pump based on heart rate. *American Society for Artificial Internal Organs Journal*, *57*(4), 262–267. https://doi.org/10.1097/MAT.0b013e31821798aa

Coulson, J., Lygeros, J., & Dörfler, F. (2019, June). *Data-enabled predictive control: In the shallows of the DeePC*. 2019 18th European Control Conference (ECC), Naples, Italy (pp. 307–312). IEEE. https://doi.org/10.23919/ECC.2019.8795639

dos Santos Coelho, L., Wicthoff, M. P., Sumar, R. R., & Coelho, A. A. R. (2010). Model-free adaptive control design using evolutionary-neural compensator. *Expert Systems with Applications*, *37*(1), 499–508. https://doi.org/10.1016/j.eswa.2009.05.042

Fliess, M., & Join, C. (2013). Model-free control. *International Journal of Control*, *86*(12), 2228–2252. https://doi.org/10.1080/00207179.2013.810345

Fliess, M., Join, C., & Sira-Ramírez, H. (2008). Nonlinear estimation is easy. *International Journal of Modelling Identification Control*, *4*(1), 12–27. https://doi.org/10.1504/IJMIC.2008.020996

Fliess, M., Lévine, J., Martin, P., & Rouchon, P. (1995). Flatness and defect of non-linear systems: Introductory theory and examples. *International Journal of Control*, *61*(6), 1327–1361. https://doi.org/10.1080/00207179508921959

Garone, E., & Nicotra, M. M. (2016). Explicit reference governor for constrained nonlinear systems. *IEEE Transactions on Automatic Control*, *61*(5), 1379–1384. https://doi.org/10.1109/TAC.2015.2476195

Hamrah, R., & Sanyal, A. K. (2020). Finite-time stable tracking control for an underactuated system in SE(3) in discrete time. *International Journal of Control*, to appear. https://doi.org/10.1080/00207179.2020.1841299

Hamrah, R., Sanyal, A. K., & Prabhakaran Viswanathan, S. (2019). *Discrete finite-time stable position tracking control of unmanned vehicles*. 2019 IEEE 58th Conference on Decision and Control (CDC), Nice, France (pp. 7025–7030). IEEE. https://doi.org/10.1109/CDC40024.2019.9029700

He, X., & Asada, H. (1993, June). *A new method for identifying orders of input-output models for nonlinear dynamic systems*. 1993 American Control Conference, San Francisco, CA (pp. 2520–2523). IEEE. https://doi.org/10.23919/ACC.1993.4793346

Keel, L. H., & Bhattacharya, S. P. (2017). Controller synthesis free of analytical models: Three term controllers. *IEEE Transactions on Automatic Control*, *53*(6), 1353–1369. https://doi.org/10.1109/TAC.2008.925810

Killingsworth, N. J., & Krstic, M. (2006). PID tuning using extremum seeking: Online, model-free performance optimization. *IEEE Control Systems Magazine*, *26*(1), 70–79.https://doi.org/10.1109/MCS.2006.1580155

Lyapunov, A. M. (1992). *The general problem of the stability of motion* (A. T. Fuller, Trans.). Taylor & Francis.

Mboup, M., Join, C., & Fliess, M. (2009, April 1). Numerical differentiation with annihilators in noisy environment. *Numerical Algorithms*, *50*(4), 439–467. https://doi.org/10.1007/s11075–008-9236–1.

Novara, C., & Formentin, S. (2018). Data-driven inversion-based control of nonlinear systems with guaranteed closed-loop stability. *IEEE Transactions on Automatic Control*, *63*(4), 1147–1154. https://doi.org/10.1109/TAC.2017.2744499

Polóni, T., Kalabić, U., McDonough, K., & Kolmanovsky, I. (2014). *Disturbance canceling control based on simple input observers with constraint enforcement for aerospace applications*. 2014 IEEE Conference on Control Applications (CCA), Juan Les Antibes, France (pp. 158–165). IEEE. https://doi.org/10.1109/CCA.2014.6981345

Polóni, T., Kolmanovsky, I., & Rohal'-Ilkiv, B. (2017, September). Simple input disturbance observer-based control: Case studies. *Journal of Dynamic Systems, Measurement, and Control*, *140*(1), 014501. https://doi.org/10.1115/1.4037298

Ren, Q., & Bigras, P. (2017). A highly accurate model-free motion control system with a Mamdani fuzzy feedback controller combined with a TSK fuzzy feed-forward controller. *Journal of Intelligent & Robotic Systems*, *86*(3), 367–379. https://doi.org/10.1007/s10846-016-0448-7

Rhodes, C., & Morari, M. (1998). Determining the model order of nonlinear input/output systems. *AIChE Journal*, *44*(1), 151–163. https://doi.org/10.1002/aic.690440116

Roman, R. C., Radac, M. B., Precup, R. E., & Petriu, E. M. (2017). Virtual reference feedback tuning of model-free control algorithms for servo systems. *Machines*, *5*(4), 25. https://doi.org/10.3390/machines5040025

Sanyal, A. K., Warier, R. R., & Hamrah, R. (2019, June). *Finite time stable attitude and angular velocity bias estimation for rigid bodies with unknown dynamics*. 2019 18th European Control Conference (ECC), Naples, Italy (pp. 4047–4052). IEEE. https://doi.org/10.23919/ECC.2019.8796262

Sanyal, A. K., Warier, R. R., & Viswanathan, S. P. (2019). Finite time stable attitude estimation of rigid bodies with unknown dynamics. *Asian Journal of Control*, *21*(6), 3926–3931. https://doi.org/10.1002/asjc.2089

Syafiie, S., Tadeo, F., Martinez, E., & Alvarez, T. (2011). Model-free control based on reinforcement learning for a wastewater treatment problem. *Applied Soft Computing*, *11*(1), 73–82. https://doi.org/10.1016/j.asoc.2009.10.018

Tabuada, P., & Fraile, L. (2019, December). *Data-driven control for SISO feedback linearizable systems with unknown control gain*. 2019 IEEE 58th Conference on Decision and Control (CDC), Nice, France (pp. 1803–1808). IEEE. https://doi.org/10.1109/CDC40024.2019.9029987

Tabuada, P., Ma, W. L., Grizzle, J., & Ames, A. (2017, December). *Data-driven control for feedback linearizable single-input systems*. 2017 IEEE 56th Annual Conference on Decision and Control (CDC), Melbourne, VIC, Australia (pp. 6265–6270). IEEE. https://doi.org/10.1109/CDC.2017.8264603

Trapero, J. R., Sira-Ramírez, H., & Battle, V. F. (2007). A fast on-line frequency estimator of lightly damped vibrations in flexible structures. *Journal of Sound and Vibration*, *307*(1–2), 365–378. https://doi.org/10.1016/j.jsv.2007.07.005

Vidyasagar, M. (2002). *Nonlinear systems analysis* (2nd ed.). SIAM.

Villagra, J., & Balaguer, C. (2011). A model-free approach for accurate joint motion control in humanoid locomotion. *International Journal of Humanoid Robotics*, *8*(1), 27–46. https://doi.org/10.1142/S0219843611002332

Viswanathan, S. P., Sanyal, A. K., & Warier, R. R. (2017). *Finite-time stable tracking control for a class of underactuated aerial vehicles in SE(3)*. 2017 American Control Conference (ACC), Seattle, WA (pp. 3926–3931). IEEE. https://doi.org/10.23919/ACC.2017.7963556

Wang, N., Hamrah, R., & Sanyal, A. K. (2019). *A finite-time stable observer for relative attitude estimation*. 2019 IEEE 58th Conference on Decision and Control (CDC), Nice, France (pp. 7911–7916). IEEE. https://doi.org/10.1109/CDC40024.2019.9029806

Younes, Y. A., Drak, A., & Noura, H. (2016). Robust model-free control applied to a quadrotor UAV. *Journal of Intelligent & Robotic Systems*, *84*(1), 37–52. https://doi.org/10.1007/s10846-016-0351-2